JOURNAL OF CATALYSIS 116, 556–567 (1989)

Hydrocarbon Surface Fragments over Co/SiO_2: An FTIR Study

KEITH G. ANDERSON[1] AND JOHN G. EKERDT

Department of Chemical Engineering, The University of Texas at Austin, Austin, Texas 78712

Received August 2, 1988; revised November 16, 1988

Linear butenes and ethylene were adsorbed onto Co/SiO_2, which was 80% reduced, and the resulting surface species were analyzed with Fourier-transform infrared spectroscopy. Group frequency comparison with liquid alkane data and consideration of the effect of the surface selection rule on mode intensities are used to argue for the formation of 2,3-dimetallabutane, 1,1,2-trimetallabutane, and 1,1,3-trimetallabutane from the linear butenes. The ethylene results are consistent with the formation of ethylidyne. Hydrogenation and temperature-programmed desorption studies were also performed to determine the reactivity of the C_4 species formed during adsorption. Hydrogenation led to *n*-butane in the gas phase and to the formation of a terminally bonded surface species that is suggested to be butylidyne. Programmed heating resulted in the transformation of the 2,3 and/or 1,1,2 species into the 1,1,3 species by 42°C, followed by the evolution of gas-phase *n*-butane above 60°C. Above 90°C, C–C scission products were observed. The infrared results over Co are compared to previous studies over Ni.

I. INTRODUCTION

Vibrational spectroscopies which allow the direct examination of surfaces complexes have proven effective in studying heterogeneous catalysis (*1*). Fourier-transform infrared spectroscopy (FTIR) has been particularly useful with supported metal catalysts because it permits the rapid collection of high resolution spectra of surface species at moderate pressures (*2*). For example, IR spectroscopy has been used to characterize adsorbed butenes over Ni/SiO_2 (*3*) and adsorbed ethylene over alumina-supported Pt, Rh, Pd, Ru (*4*), and Ni (*5*), and silica-supported Pt and Pd (*6*). A recent *in situ* IR study has shown that ethylidyne is not an intermediate in ethylene hydrogenation over Pd/Al_2O_3 at 300°K (*7*).

The majority of the hydrocarbon IR studies have been conducted with Ni (*3, 5, 8–17*) and Pt (*4, 9, 15, 16, 18*). Much less has been reported over Co (*11, 12, 19*). Cobalt is interesting because its catalytic chemistry differs from Ni and Pt. Cobalt is also interesting because the crystalline structure for dispersed Co differs from the structure for bulk Co (*20*); thus, it is particularly important to study Co in the dispersed form. In the hydrogenolysis reaction, single bond rupture occurs over Pt, alkanes undergo sequential loss of methylene from a terminally bound alkyl over Ni, and deep fragmentation of adsorbed species occurs over Co (*21*). These catalysts also differ considerably in their activity and selectivity for carbon monoxide hydrogenation (*22*) and in their activity for hydrogenation and H–D exchange (*23*). By studying the spectra of adsorbates on the surface of Co and their transformations we had hoped to understand better the catalytic differences between these three metals. Linear butenes and ethylene were chosen as model adsorbates because they have been studied over Pt and Ni, affording a comparison. Silica was used as the support because of the greater reducibility of Co over silica than over alumina (*24*).

II. METHODS

Transmission IR spectra were collected on a Bio-Rad/Digilab FTS 15-90 spectrome-

[1] Present address: Ethyl Corp., P.O. Box 341, Baton Rouge, LA 70821.

0021-9517/89 $3.00

ter set at a resolution of 2 cm^{-1}. Typically 100 scans were collected which required 1 to 1.5 min. A 19 mW Hi-temp source and an MCT detector were used to maximize the sensitivity of the instrument over the spectral range of 3300 to 500 cm^{-1}. It was possible with this system to observe signals as low as 0.001 absorbance units (AU) while passing the beam through catalyst samples that adsorbed as much as 50% of the incident light.

A glass IR cell (*25*) was used for the butene studies and a stainless-steel cell (*3*) was used for the ethylene studies. The 9.5 wt% Co/SiO_2 catalyst was prepared by impregnation of silica (Cab-O-Sil HS-5, Cabot Corp., 325 m^2 g^{-1}) with cobaltous nitrate hexahydrate (Puratronic grade 99.999%, Johnson Matthey). A reduction procedure similar to that of Bartholomew and coworkers (*24*, *26*) was used to reduce the cobalt.

During a typical butene IR experiment, 60 mg of reduced catalyst was pressed into a thin, 2.54-cm diameter disk and loaded into the cell sample holder. The cell was evacuated with a mechanical pump (5 mTorr) for 5 to 30 min to remove water from the disk and then 50 to 60 cm^3 min^{-1} of hydrogen was passed over the disk as the temperature was raised to 400°C at 5°C min^{-1}. Temperature was held at 400°C for 0.5 to 2 hr to remove surface oxide from the catalyst. The disk was then cooled to room temperature in flowing hydrogen and lowered into the IR beam path. Just prior to the adsorption of the olefins, the cells was evacuated (5 mTorr) for 1 min to remove hydrogen from the gas phase (*3*). The catalyst was still "hydrogen covered" (*8*). (Hydrogen chemisorption experiments established that approximately 70% of a monolayer of hydrogen remained on the Co following this evacuation.) A linear butene was then added to the gas phase via syringe injection to produce 20 Torr of pressure in the cell. After a dosing period of 5 to 15 min, the gas phase was sampled for analysis on a gas chromatograph (GC). The cell was subsequently evacuated (5 mTorr) for 1 min and IR spectra collection was initiated, with the cell maintained under static vacuum; these spectra are referred to as the initially adsorbed spectra. Additional spectra were collected following exposure of the catalyst to 60 Torr of hydrogen. New catalyst samples were used for each experiment.

The ethylene experimental conditions are described elsewhere (*5*). Following the same *in situ* reduction process described above the disk was cooled to −45°C in flowing hydrogen and the cell was evacuated (5 mTorr) for 1 min to generate the hydrogen-covered surface. Five Torr of ethylene was added to the cell and after 20 min the cell was evacuated for 1 min (5 mTorr) and maintained under static cell vacuum while spectra were collected.

The system used for the temperature-programmed desorption (TPD) work is illustrated in Fig. 1. It consisted of a gas manifold section, quartz reactor bed, 16-loop gas sample valve, and data acquisition system. Effluent samples collected in the sample loops were analyzed on a 23% SP-1700 on 80/100 mesh Chromosorb PAW stainless-steel column (9 m × 3.2 mm o.d.) or an alumina-packed capillary column (Chromopak 50 m × 0.53 mm i.d. PLOT Al_2O_3/KCl).

Catalyst Characterization

The chemisorption apparatus used to determine catalyst dispersion and the degree of Co reduction has been previously described (*3*). A pressure decreasing technique similar to that of Reuel and Bartholomew (*24*) was used to calculate the monolayer coverage of hydrogen on the surface and the percentage reduction of the metal.

Electron microscopy of the catalyst was carried out on a Siemens Elmskop I electron microscope to determine the crystallite distribution. Micrograph samples were prepared by spraying a fine mist of suspended catalyst particles onto a carbon-covered

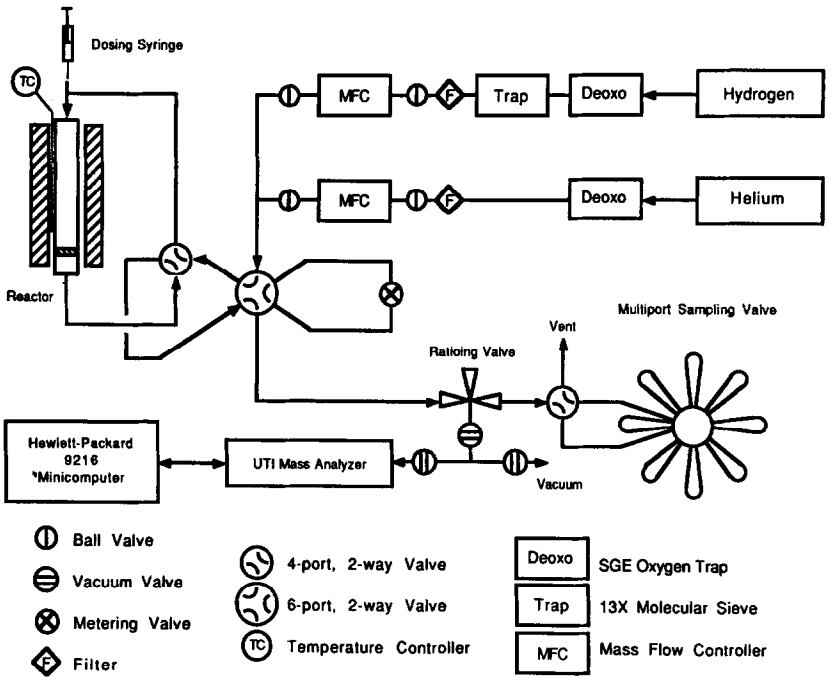

FIG. 1. Temperature-programmed desorption system schematic.

grid. Photomicrographs were taken at a magnification of 48,000X and subsequently photoenlarged to 190,000 to 220,000X during printing. At these magnifications, particles larger than about 10 Å could be distinguished from the support and carbon film. Confirmation of the crystallinity of some of the larger particles was made through dark field illumination techniques.

A summary of the characterization results is presented in Table 1.

TABLE 1

Catalyst Characteristics

Crystallite diameter[a]	93 Å
Dispersion[b]	10.3%
Reduction[c]	81.0%
Weight loading[d]	9.51%

[a] Surface-averaged diameter calculated from the electron microscopy results.

[b] Calculated from the electron microscopy results.

[c] Based on O_2 titration at 375°C.

[d] Analysis performed by Radian Corp.

Materials

Hydrogen (99.999% Big Three) and helium (99.995%) were passed through oxygen traps and 13X molecular sieves (both Scientific Glass Engineering) before being used. All the adsorbate gases, 1-butene (99.9% Matheson), *trans*-2-butene (99.4% Union Carbide), *cis*-2-butene (96.0% Union Carbide), and ethylene (99.99% Matheson) were used without further purification.

III. RESULTS

The experiments with Co were performed in a manner similar to those conducted over 8.29 wt% Ni/SiO_2 (*3*) so that a comparison between the metals could be made. Cobalt presented more problems experimentally because of the difficulty in reducing the raw catalyst, $Co(NO_3)_2 \cdot (H_2O)_x/SiO_2$, to Co/SiO_2 (at best 80% of the cobalt was reduced) and maintaining the surface free of an oxide overlayer beyond that present at 80% reduction. X-ray diffraction

established that the reduced catalyst was oxidized to the cobalto–cobaltic oxide (Co_3O_4) rather than cobaltous oxide (CoO) at room temperature, if exposed to air.

It was not possible to establish the available fraction of the surface that was reduced or the nature of the surface oxide present at 80% reduction. The extreme sensitivity of the catalyst to O_2 contamination, the similarity of the results to other metals (see under Discussion), and blank experiments over a fully oxidized catalyst are used to propose that the spectra and results reflect the interaction of the hydrocarbons with cobalt metal. In one experiment the catalyst was made inactive by exposing a disk (96 μmole Co) to 10 μl of hydrocarbon-free air (0.086 μmole O_2) at room temperature following the usual reduction. About 5 μmole O_2 would have been required to oxidize the entire surface to Co_3O_4; therefore, Co metal was probably also present on this disk following exposure to O_2. This disk was subsequently exposed to 1-butene. Less than 10% of the 1-butene reacted. The gas-phase composition was 1-butene (90%), *n*-butane (2.3%), *trans*-2-butene (3.7%), and *cis*-2-butene (2.7%). No IR evidence of hydrocarbon species on the surface existed after 1 min of evacuation of the gas phase, and only a very minor peak (0.0020 AU) appeared at 2958 cm^{-1} following the addition of hydrogen.

Blank experiments were carried out to test the adsorption of butenes on silica alone. Negligible absorbance bands (<0.0025 AU) were observed at 2968 and 2925 cm^{-1} on the surface following 1 min of evacuation of a standard dose of 1-butene. No reaction products were found in the gas phase using GC.

Room Temperature Adsorption of Linear Butenes

The spectra of initially adsorbed 1-, *trans*-2- and *cis*-2-butene are presented in Fig. 2. The spectra from these compounds were very similar to each other with the main absorbance bands located near 2965, 2932, 2872, 1458, and 1380 cm^{-1}. Peak height intensities and mode assignments, based on liquid alkane data, are given in Table 2. Table 3 presents a component analysis and distribution of the gas-phase reaction products following the 15-min dosing period. No C–C bond scission products were found under these conditions, nor were there any signs of skeletal rearrange-

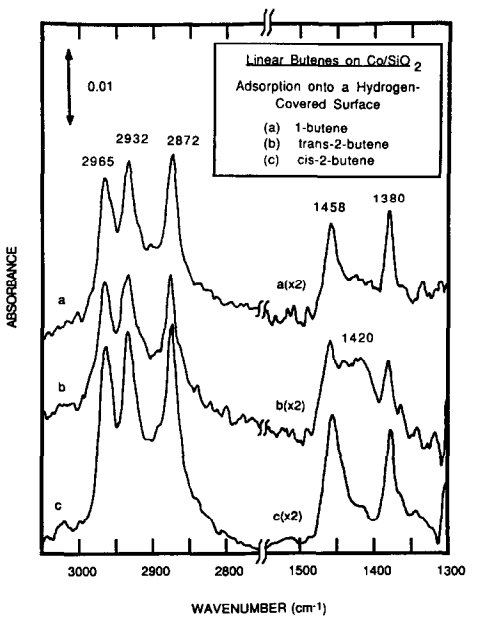

FIG. 2. Linear butene adsorption on a hydrogen-covered surface of Co/SiO_2 at 28°C, 20 Torr total pressure; (a) 1-butene, (b) *trans*-2-butene, and (c) *cis*-2-butene.

TABLE 2

Group Assignments and Observed Peak Intensities for Initial Dosing of Butenes onto Hydrogen-Covered Cobalt[a]

Group	Mode	Frequency	1-Butene	*trans*-2-Butene	*cis*-2-Butene
CH_3	ν_{as}	2960 ± 8	1.97	1.77	2.68
	ν_{sy}	2874 ± 4	2.16	1.94	3.03
	δ_{as}[b]	1461 ± 7	0.56	0.64	0.91
	δ_{sy}	1372 ± 10	0.60	0.57	0.76
CH_2	ν_{as}	2926 ± 6	2.16	1.89	2.91
	ν_{sy}	2856 ± 6	0.41	0.42	0.61
	δ[b]	1461 ± 7	0.56	0.63	0.91

[a] Intensities in absorbance units × 100.
[b] $\delta_{as}(CH_3)$ and $\delta(CH_2)$ are usually unresolved.

TABLE 3

Gas Phase Products following Initial Dosing of Butenes (Carbon Mole Percent)

Gas phase component	Gas dosed		
	1-Butene	*trans*-2-Butene	*cis*-2-Butene
Methane	0	0	0
C_2[a]	0.1	0	0
Propane	t[b]	0	0
Propene	t	0	t
Isobutane	t	0	0
n-Butane	1.41	1.19	1.63
Isobutene	0	0	0
1-Butene	78.14	2.49	3.25
t-2-Butene	10.34	79.77	51.60
c-2-Butene	10.06	16.56	43.98
Butadiene	0	0	0

[a] Ethane and ethylene were not always resolved.
[b] Less than 0.1 mole%.

ment in the product spectrum. (The C_1–C_3 compounds were found to be impurities in the adsorbed gas.) Gas-phase analysis of oligomerization products (C_8) showed that the carbon conversion to octane was 0.3%.

Examination of the gas phase present in the cell with IR showed that rapid changes in the gas-phase composition were completed within 5 min of dosing 1-butene. The gas-phase composition had not reached equilibrium (*trans*-2-butene 77%, *cis*-2-butene 20%, 1-butene 3%) after 15 min, when gas samples were taken from the IR cell (Table 3). Because of the large dead volume of the cell, kinetic analysis of the gas-phase products was not possible.

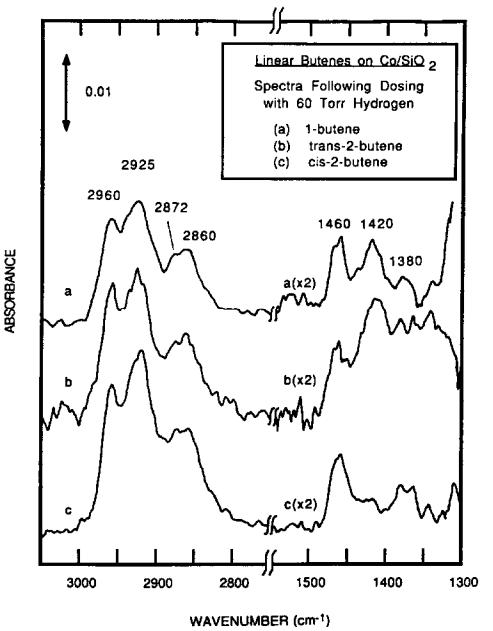

FIG. 3. Spectra of linear butenes recorded following exposure to 60 Torr of hydrogen; (a) 1-butene, (b) *trans*-2-butene, and (c) *cis*-2-butene.

Following collection of the spectra in Fig. 2, 60 Torr of hydrogen was added to the IR cell, held for 15 min, then evacuated from the cell (5 mTorr). *n*-Butane was the only product found in the gas phase, suggesting that no hydrogenolysis of the C_4 backbone occurred. After the addition and evacuation of hydrogen, the absorption bands (Fig. 3) appeared broader and the intensity of the bands near 2872 and 1380 cm^{-1} was weaker. The 2965- and 2932-cm^{-1} bands shifted slightly to lower wavenumbers. There was also a new band near 2860 cm^{-1} and a broad absorbance near 1420 cm^{-1} became prominent in the C–H deformation region. Mode assignments and peak intensities are presented in Table 4.

The effect of evacuation upon the initially adsorbed species is shown in Fig. 4. There was a definite decline in the 2930 and 2870 cm^{-1} peaks for 1-butene following 15 min of dynamic vacuum (5 mTorr) versus 1 min of evacuation (Spectrum 4a). In the C–H deformation region, the 1380-cm^{-1} peak was observed to decline while the broad absorbance at 1420 cm^{-1} increased by 100%.

TABLE 4

Group Assignments and Observed Peak Intensities for Hydrogenated Surface Species[a]

Group	Mode	Frequency	1-Butene	*trans*-2-Butene	*cis*-2-Butene
CH_3	ν_{as}	2960 ± 8	1.34	1.81	1.93
	ν_{sy}	2874 ± 4	0.80	1.03	1.31
	δ_{as}[b]	1461 ± 7	0.42	0.42	0.46
	δ_{sy}	1372 ± 10	0.25	0.32	0.25
CH_2	ν_{as}	2926 ± 6	1.54	2.01	2.35
	ν_{sy}	2856 ± 6	0.83	0.99	1.31
	δ[b]	1461 ± 7	0.42	0.42	0.46

[a] Intensities in absorbance units ×100.
[b] $\delta_{as}(CH_3)$ and $\delta(CH_2)$ are usually unresolved.

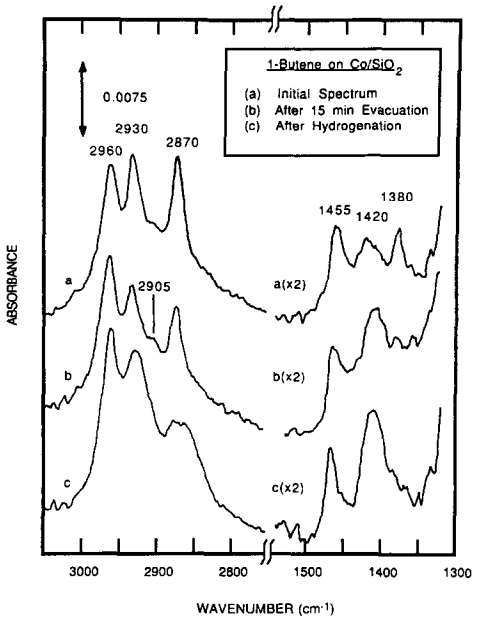

FIG. 4. 1-Butene adsorption at 28°C on a hydrogen-covered surface of Co/SiO_2 and subsequently evacuated for 15 min and then hydrogenated. (a) Adsorption followed by 1 min evacuation; (b) subsequent evacuation for an additional 15 min; (c) exposure to 60 Torr of hydrogen.

Frequency shifts due to evacuation were less than 4 cm^{-1}. Upon addition of 60 Torr of hydrogen, the total integrated spectral intensity increased, but the resulting peaks (Fig. 4) did not resemble those produced by hydrogen treatment of the initially adsorbed species (Fig. 3). Instead of the absorbance near 2930 cm^{-1} being the most intense, the 2960-cm^{-1} band became most intense. In the bending region, the large peak at 1420 cm^{-1} completely dominated the spectrum. Analysis of the gas phase following hydrogen addition showed that *n*-butane had formed. (Some 1-butene was also observed in the gas phase, but this was probably due to syringe contamination.)

Temperature Effects

Figure 5 presents infrared intensity changes that occurred during heating the initial species that formed from 1-butene under static vacuum in the glass IR cell. Only data from the stretching region are presented because silica absorbance bands increased considerably with temperature in the C–H deformation region, making it too difficult to determine changes in the 1420- and 1380-cm^{-1} absorbance intensities. The absorbance intensity at 2872 cm^{-1} declined upon heating until the sample reached 42°C. Conversely, the other two major bands in the stretching region grew in intensity until, at about the same temperature, they also ceased to change. All the absorbances remained relatively constant between 42 and approximately 60°C, at which point there was a decline in intensity of the 2872-cm^{-1} band. Above 70°C the other bands decreased in intensity. The heating was stopped at 85°C to prevent decomposition of the optic sealant.

The TPD spectrum of 1-butene adsorbed onto Co/SiO_2 is given in Fig. 6. (A much faster heating rate was used for the TPD results presented in Fig. 6 than was used for the IR results presented in Fig. 5.) The upper part of this figure contains the continuous intensities for masses 2, 41, 56, and 58 which correspond to hydrogen, propane, butene, and *n*-butane, respectively. Temperature and GC data for the effluent composition with time are presented in the lower portion of Fig. 6. Three desorption

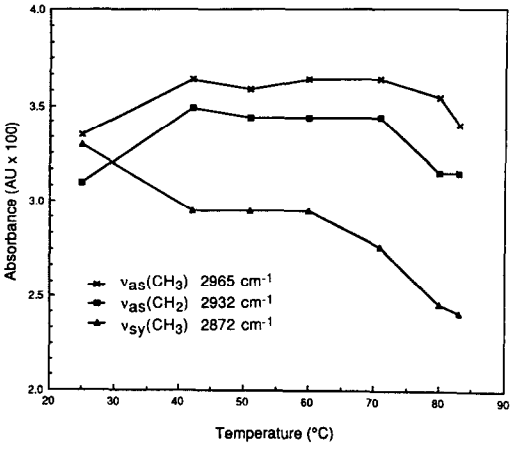

FIG. 5. Absorbance intensities versus temperature as the catalyst was heated under vacuum following the adsorption of 1-butene.

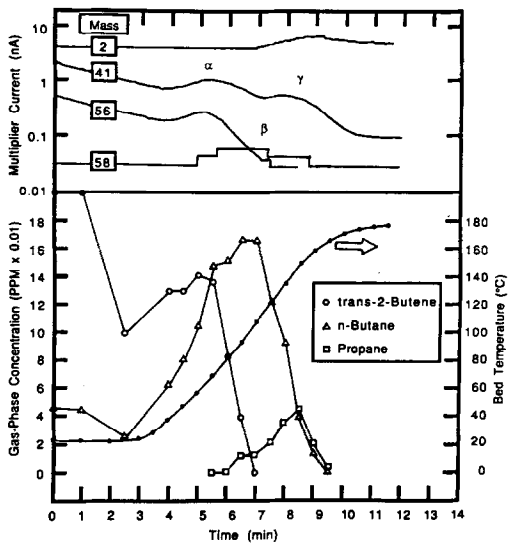

FIG. 6. Temperature-programmed desorption results for 1-butene dosed at 28°C. The upper figure presents mass spectrometer electron multiplier currents for the selected masses. The lower figure presents the gas phase concentrations determined by GC.

peaks, α, β, and γ, were observed with starting temperatures of about 30, 50, and 110°C, respectively. The α peak was composed of C_4 butenes (only *trans*-2-butene is presented in Fig. 6). The β peak corresponded to *n*-butane. The γ peak was composed of scission products of the adsorbed species, mostly propane and methane. Blank experiments with silica demonstrated that the α peak was due to residual butene absorbed on the silica.

Absorption of Ethylene

The spectrum following the adsorption of ethylene onto Co/SiO_2 at −45°C is presented in Fig. 7a. A simple spectrum resulted with intense absorbances at 2880 and 1347 cm^{-1}. This temperature was selected so that the Co results could be directly compared to previous work over Ni/Al_2O_3 (*5*) and Ni/SiO_2 (*27*).

IV. DISCUSSION

Ideally, deuterated compounds, normal coordinate analysis, group frequencies, and comparisons with organic and organometallic compounds should be used in the assignment of IR bands to surface structures. Deuterated butenes were not used in this study because of the potential problems with H–D scrambling (*28, 29*). Normal coordinate analysis requires knowledge of the symmetry and structure of the proposed surface species and the symmetry of the adsorption site (*30*). The uncertainty in adsorption site, caused by the presence of several crystalline planes on a supported metal (*31*), coupled with the loss of information below 1300 cm^{-1} by the silica support make normal coordinate analysis impractical. This leaves the group frequency approach and comparisons with organic and organometallic spectra as the chief means of interpreting the IR spectra of surface species. The group frequency technique is particularly well suited for hydro-

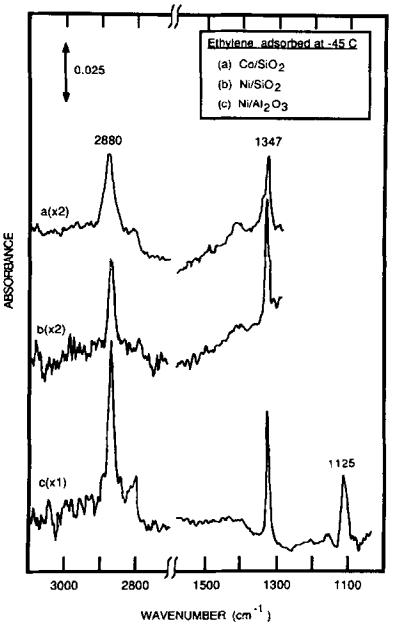

FIG. 7. Infrared spectra of ethylene adsorbed at −45°C and an ethylene dosing pressure of 50.0 ± 1.2 Torr for 15 min. (a) Hydrogen-covered 9.5 wt% Co/SiO_2, (b) hydrogen-covered 9 wt% Ni/SiO_2 (from Ref. (*27*)), and (c) hydrogen-covered 9 wt% Ni/Al_2O_3 (reproduced, by permission of the publisher from Ref. (*5*)).

TABLE 5

Mode Intensity Ratios of Initially Formed Species Based on Alkane Assignments

Ratio	Expected[a]	1-Butene	*trans*-2-Butene	*cis*-2-Butene
$\nu_{as}/\nu_{sy}(CH_3)$	2.3	0.91	0.91	0.88
$\nu_{as}/\delta_{sy}(CH_3)$	6.3	3.3	3.1	3.5
$\nu_{as}/\nu_{sy}(CH_2)$	1.7	4.8	4.5	5.3

[a] See text.

carbons since the hydrogen atoms are much lighter than the carbon atoms, localizing vibrations to the carbon–hydrogen bonds on different functional groups of the molecule. In addition, all internal C–H modes for sp^3-hybridized species can be observed above the silica cutoff at 1300 cm^{-1}.

Initial Spectra for the Linear Butenes

No bands appeared in the spectra where fundamental or overtone vibrations were expected for *sp*- or sp^2-hybridized carbon. All adsorbed species are assumed to be sp^3-hybridized. The mode assignments given in Tables 2 and 4 were based solely on liquid alkane data. These mode assignments follow closely those of Morrow and Sheppard (*9*) and Campione and Ekerdt (*3*). Because of the lack of C–C bond scission, skeletal isomerization, and the small amount of dimerization (0.3%), it is reasonable to conclude that the carbon backbone of the linear butenes remained intact during adsorption, reaction, and desorption over Co/SiO_2 at room temperature.

The effect of the surface selection rule (*32*) must be considered when proposing structures from the mode assignments in our system (*25*). Table 5 gives the intensity ratios of different modes of the same functional group for the initially formed species. Because surface selection enhances the intensity of modes whose dipole moments are perpendicular to the metal surface, these mode ratios provide information about the orientation of functional groups with respect to the surface. Campione and Ekerdt (*3*) applied the surface selection rule when accounting for the intensity ratios which were observed versus ratios that were expected. Similar reasoning applied to the values in Table 5 leads to the conclusion that, for the initially formed species, the symmetric methyl mode was enhanced and the C_{3v} axis of rotation for the methyl group would have to be oriented close to perpendicular to the metal surface, and the asymmetric mode of the methylene group was enhanced and that most of the methylene groups were oriented with the C_{2v} axis of rotation parallel to the surface of the metal (*33*).

The spectra observed for 1-butene adsorption over silica-supported Co, Ni (*3*), and Pt (*9*) are presented in Fig. 8. The absorbance locations and the relative intensities of the bands are similar over the three metals. The interpretation given here and in Ref. (*3*) is a possible alternative to that provided by Morrow and Sheppard (*9*). (Many of the details will not be repeated here but may be found elsewhere (*3*, *25*).)

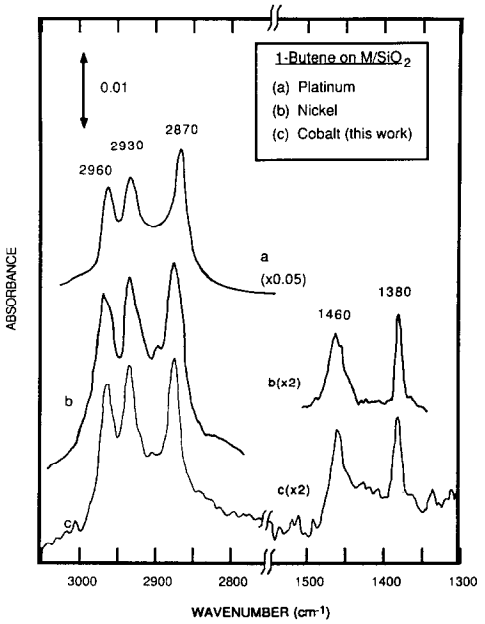

FIG. 8. Infrared spectra following 1-butene adsorption over silica-supported metals. (a) Adsorption at 20°C on 16 wt% Pt/SiO_2 (reproduced by permission of the publisher from Ref. (*9*)), (b) adsorption at 28°C on 8.3 wt% Ni/SiO_2 (from Ref. (*3*)), and (c) adsorption at 28°C on 9.5 wt% Co/SiO_2 (this work).

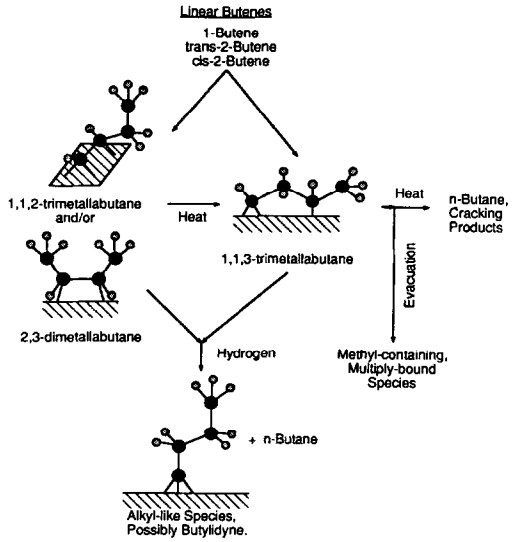

FIG. 9. Proposed scheme for the adsorption and reaction of linear butenes over Co/SiO_2.

Morrow and Sheppard accounted for the lack of $\nu_{sy}(CH_2)$ intensity by proposing that the $\nu_{sy}(CH_2)$ mode was present but was hidden under the low frequency tail of the 2872-cm^{-1} band. The extra absorbance in the band at 2872 cm^{-1} ($\nu_{sy}(CH_3)$) was accounted for as being due to the CH_2M group in a four-membered strained ring, as per their assignment for an associatively adsorbed ethylene species (*15*). The extra intensity of the $\nu_{as}(CH_2)$ mode around 2930 cm^{-1} was rationalized as being due to an additional contribution from a —CHM- group. The entire spectrum was attributed to a single species, associatively adsorbed 1,2-dimetallabutane.

We propose that the linear butenes adsorbed over Co/SiO_2 and Ni/SiO_2 at room temperature formed at least two surface species, one with enhanced symmetric methyl modes and one with enhanced asymmetric methylene modes. Three surface species may be postulated, 2,3-dimetallabutane, 1,1,2-trimetallabutane, and 1,1,3-trimetallabutane, and are pictured in Fig. 9. The 2,3 and 1,1,2 species, with their methyl groups pointing away from the surface, could account for the enhancement in the symmetric methyl modes. The 1,1,2-trimetallabutane shown in Fig. 9 differs from the conformer proposed by Campione and Ekerdt (*3*) in that the structure shown here has the methyl group pointing away from the surface. This particular conformer would be favored as steric hindrance of the methyl group with the metal surface would be minimized; thus, its contribution to the infrared spectra would be significant. The 1,1,2 species is also consistent with the weak $\nu_{sy}(CH_2)$ mode. Calculation of the absorbance due to this mode (*25*) showed that, due to the action of the surface selection rule, the $\nu_{sy}(CH_2)$ mode would be weak and could be hidden under the tail of the $\nu_{sy}(CH_3)$ band near 2870 cm^{-1}. The spectra observed initially (Fig. 2) were consistent with the formation of either the 2,3-dimetallabutane and/or the 1,1,2-trimetallabutane. The 1,1,3 species, with the methylene group pointing away from the surface, could account for the enhancement in the asymmetric methylene mode and is also proposed to form upon adsorption.

Spectra following Hydrogenation

With the exception of the band at 1420 cm^{-1}, the spectra (Fig. 3) resulting from exposure of the surface species to 60 Torr of hydrogen were very similar. (The band at 1420 cm^{-1} is believed to be due to another species.) There was a 30–40% decline in the intensity of the bands at 2872 and 1380 cm^{-1}, while at the same time the $\nu_{sy}(CH_2)$ band at 2860 cm^{-1} became well resolved. Absorbance intensity ratios following hydrogenation (Table 6) changed from the val-

TABLE 6

Mode Intensity Ratios of Hydrogenated Species Based on Alkane Assignments

Ratio	Expected[a]	1-Butene	*trans*-2-Butene	*cis*-2-Butene
$\nu_{as}/\nu_{sy}(CH_3)$	2.3	1.7	1.8	1.5
$\nu_{as}/\delta_{sy}(CH_3)$	6.3	5.5	5.7	7.7
$\nu_{as}/\nu_{sy}(CH_2)$	1.7	1.9	2.0	1.8

[a] See text.

ues for the initial adsorption spectra (Table 5). The methyl intensity ratios (Table 6) show a slight enhancement of the $\nu_{sy}(CH_3)$ mode and are nearer to the value for methyl groups in alkanes. A methyl group's absorbance intensity, for any adsorbed C_4 fragment (*3, 25*), would be influenced by the surface selection rule if it were held rigidly with respect to the surface. The change in the $\nu_{as}/\nu_{sy}(CH_3)$ intensity ratio suggests that the methyl group was free to move with respect to the surface for the adsorbed species formed during hydrogenation. This type of motion could be found in a terminally bonded structure with alkyl-like character.

Nothing definitive can be said from the data with regard to the precise manner of bonding to the surface of this terminally bonded structure. The silica support does not allow examination of the fingerprint region of the IR spectrum where metal–carbon and carbon–carbon stretches are expected to occur. The ethylene results discussed below are consistent with the formation of ethylidyne over Co. The formation of butylidyne is reported from linear butenes over Pt(111) and Rh(111) (*34, 35*). Precedence for butylidyne formation and the possibility that ethylidyne formed over Co lead us to suggest in Fig. 9 that butylidyne formed during hydrogenation. Butylidyne methylene modes are consistent with the effect of the surface selection rule. For the β carbon, the $\nu_{as}(CH_2)$ mode would be attenuated and the $\nu_{sy}(CH_2)$ mode dipole moment would have components parallel and perpendicular to the surface. The intensities of the $\nu_{as}(CH_2)$ and $\nu_{sy}(CH_2)$ modes for the γ carbon would change as the orientation of the methyl group C_{3v} axis of rotation changed with respect to the surface.

Effect of Temperature

By means of a material balance, it is possible to show that the gas-phase concentration of a desorbing species is proportional to the rate of change in the surface concentration of the corresponding adsorbed species. Since the observed IR intensity of a surface species is proportional to its surface concentration by Beer's law, inflection points in the intensity data of Fig. 5 should correspond to maxima in the TPD data if the IR intensity changes are due to desorption. Only two possible inflection points are found in the intensity data of Fig. 5, between 25 and 40°C and between 60 and 85°C. The first inflection does not correspond to any of the desorption peaks observed in the TPD experiment and so was not due to desorption. The second inflection point could relate to either the α or the β peaks (Fig. 6), since their maxima were near 60 and 90°C, respectively. Because the α peak was also produced in silica blank experiments, the β desorption peak corresponded to the intensity changes on the metal surface above 60°C. Thus much of the intensity loss in the infrared spectrum above 60°C was due to desorption of surface species as *n*-butane. It is also possible that some of the loss in intensity of the surface species with heating may have been due to the formation of hydrogen-deficient species (*3*).

The γ desorption peak in Fig. 6, which was caused by the C–C scission products, was not associated with changes in the IR intensities of Fig. 5. The IR experiment was terminated below the onset of the γ peak (110°C).

The species that reacted to butane in the TPD experiment were not revealed by the IR data. The intensity changes in Fig. 5 below 40°C suggest a transformation from the $\nu_{sy}(CH_3)$-enhanced species into the $\nu_{as}(CH_2)$-enhanced species (1,1,3-trimetallabutane) as shown in Fig. 9. It was probably the 1,1,3-trimetallabutane that gave rise to butane in the gas phase because an infection point in the intensity data between 60 and 85°C correlates with the maximum in the butane desorption peak.

Spectra following Evacuation

Intensity losses (Fig. 4) in the $\nu_{as}(CH_2)$, $\nu_{sy}(CH_3)$, and $\delta_{sy}(CH_3)$ modes following 15

min of evacuation are consistent with the partial desorption or reaction of the initially produced species. Reaction to a new species is supported by the growth in the 1420- and 2960-cm^{-1} absorbances as the bands associated with the initially produced species declined. Because the $\nu_{sy}(CH_2)$ mode (2860 cm^{-1}) was not observed after evacuation, the 1420- and 2960-cm^{-1} bands did not result from the terminally bonded species.

Identification of the molecular structure(s) responsible for the absorbance at 1420 cm^{-1} and the extra absorbance at 2960 cm^{-1} is not possible because of the continued presence of the initially produced species. Some of the new species formed upon evacuation apparently possessed methyl groups since the 2960-cm^{-1} absorbance was stronger than expected. Campione and Ekerdt (*3*) noted an increase in intensity of the 1420-cm^{-1} band with evacuation or heating and assigned it to the deformation vibration of a tertiary carbon atom bound to one or two metal atoms (—CHM— or —CHM_2). This undefined structure is referred to as methyl-containing, multiply bound in Fig. 9. It is shown forming from the 1,1,3 species but it may have formed from any initially formed species.

Low Temperature Adsorption of Ethylene

The ethylene experiments were performed to establish the feasibility of an alkylidyne over Co. Our interpretation is consistent with ethylidyne formation. The spectrum shown in Fig. 7a for the adsorption of ethylene at −45°C onto Co/SiO_2 is equivalent to that found for ethylene adsorption onto Ni/Al_2O_3 (*5*) and Ni/SiO_2 (*27*) with two intense bands at 2880–2870 and 1347–1340 cm^{-1}. The spectra reported in Fig. 7 were recorded under similar conditions. The alumina support permitted the additional absorbance at 1125 cm^{-1} to be detected (Fig. 7c). The 2870, 1340, and 1125 cm^{-1} absorbances over Ni/Al_2O_3 have been assigned to the $\nu_{sy}(CH_3)$, $\delta_{sy}(CH_3)$, and ν(C–C), respectively, of ethylidyne. The similarities in the spectra and conditions, combined with the formation of ethylidyne over other oxide-supported transition metals (*4*), are the reasons we suggest that ethylidyne formed over Co under our experimental conditions.

Comparison with Nickel and Platinum

The initial (Fig. 2) and hydrogenation (Fig. 3) spectra of linear butenes observed over cobalt closely resembled those found over platinum (*9*) and nickel (*3, 9*). This was surprising because these systems display very different catalytic chemistry as discussed under the Introduction. Evidently, the adsorption of linear butenes at room temperature is not sensitive to the factors that influence surface processes at catalytic conditions.

Some differences between cobalt and nickel did begin to appear upon heating adsorbed 1-butene above room temperature. Over nickel (*3*), changes in the spectra with heating were consistent with the desorption of 2,3-dimetallabutane (the $\nu_{sy}(CH_3)$-enhanced species) as *n*-butane at 40°C. Above this temperature the remaining trimetallabutane was believed to be dehydrogenated (*3*). On cobalt, the $\nu_{sy}(CH_3)$-enhanced species (2,3-dimetallabutane and/or 1,1,2-trimetallabutane) did not desorb at 40°C, but instead converted into the 1,1,3-trimetallabutane immediately upon heating. The remaining surface species did not show an *n*-butane desorption maximum until 90°C. From these data, it appears that desorption occurred readily over nickel, but over cobalt the surface species were more likely to react before desorbing. This result parallels the reactivity pattern for hydrogenolysis of alkanes over the two metals, where adsorbed species are more likely to remain and react over cobalt than over nickel (*36*).

V. SUMMARY

The results of adsorbing and reacting linear butenes over Co/SiO_2 can be rationalized in terms of the reaction scheme shown in Fig. 9. During the initial adsorption of the linear butenes, two or possibly three spe-

cies were formed. These were 1,1,3-trimetallabutane and 2,3-dimetallabutane and/or 1,1,2-trimetallabutane. The 1,1,3 species accounted for the enhancement in the $\nu_{as}(CH_2)$ mode while either the 2,3 or the 1,1,2 species accounted for the enhancement in the $\nu_{sy}(CH_3)$ mode. The 2,3 and/or the 1,1,2 species were able to convert into 1,1,3-trimetallabutane upon heating in vacuum, and at higher temperatures (60–90°C) some of the remaining surface species desorbed as *n*-butane. At still higher temperatures (ca. 100°C), C–C scission products were observed. Hydrogenation of the initially formed species led to the formation of gas-phase *n*-butane and to the formation of a terminally bonded alkyl-like species. This alkyl-like species is thought to be butylidyne because ethylidyne appeared to form from ethylene over Co/SiO_2.

ACKNOWLEDGMENTS

This work was supported by the National Science Foundation under Grant CBT-8319494. The FTIR was funded by the Department of Defense Instrumentation Grant DAAG-29-83-0097. The ethylene adsorption experiments were performed by M. P. Lapinski.

REFERENCES

1. Haller, G. T., *Catal. Rev. Sci. Eng.* **23,** 477 (1981).
2. Yates, J. T., Jr., Gelin, P., and Beebe, T., *Catal. Characterization Sci.* **35,** 404 (1985).
3. Campione, T. J., and Ekerdt, J. G., *J. Catal.* **102,** 64 (1986).
4. Beebe, T. P., Jr., and Yates, J. T., Jr., *J. Phys. Chem.* **91,** 254 (1987).
5. Lapinski, M. P., and Ekerdt, J. G., *J. Phys. Chem.* **92,** 1708 (1988).
6. Bandy, B. J., Chesters, M. A., James, D. I., McDougall, G. S., Pemble, M. E., and Sheppard, N., *Philos. Trans. R. Soc. London A* **318,** 141 (1986).
7. Beebe, T. P., Jr., and Yates, J. T., Jr., *J. Amer. Chem. Soc.* **108,** 663 (1986).
8. Eischens, R. P., and Pliskin, W. A., *in* "Advances in Catalysis" (D. D. Eley, W. G. Frankenburg, V. I. Komarewsky, and P. B. Weisz, Eds.), Vol. 10, p. 1. Academic Press, New York, 1958.
9. Morrow, B. A., and Sheppard, N., *Proc. R. Soc. London Ser. A* **311,** 415 (1969).
10. Erkelens, J., *J. Catal.* **37,** 332 (1975).
11. Soma, Y., *Bull. Chem. Soc. Japan* **50,** 2119 (1977).
12. Blyholder, G., Shihavi, D., Wyatt, W. V., and Bartlett, R., *J. Catal.* **43,** 122 (1976).
13. Pliskin, W. A., and Eischens, R. P., *J. Chem. Phys.* **24,** 482 (1956).
14. Peri, J. B., *Discuss. Faraday Soc.* **41,** 121 (1986).
15. Morrow, B. A., and Sheppard, N., *Proc. R. Soc. London Ser. A* **311,** 391 (1969).
16. Morrow, B. A., and Sheppard, N., *J. Phys. Chem.* **70,** 2406 (1966).
17. Erkelens, J., and Liefkens, Th. J., *J. Catal.* **8,** 36 (1967).
18. Soma, Y., *J. Catal.* **59,** 239 (1979).
19. Blyholder, G., and Wyatt, W. V., *J. Phys. Chem.* **78,** 618 (1975).
20. Hofer, L. J. E., and Peeples, W. C., *J. Amer. Chem. Soc.* **69,** 2497 (1947).
21. Zimmer, H., Tetenyi, P., and Paal, Z., *J. Chem. Soc. Faraday Trans. I.* **78,** 3573 (1982).
22. Vannice, M. A., *J. Catal.* **50,** 228 (1977).
23. Schuit, G. C. A., and Van Reijen, L. L., *in* "Advances in Catalysis" (D. D. Eley, W. G. Frankenburg, V I. Komarewsky, and P. B. Weisz, Eds.), Vol. 10, p. 243. Academic Press, New York, 1958.
24. Reuel, R. C., and Bartholomew, C. H., *J. Catal.* **85,** 63 (1984).
25. Anderson, K. A., Ph.D. thesis, The University of Texas at Austin, 1987.
26. Zowtiak, J. M., and Bartholomew, C. H., *J. Catal.* **83,** 107 (1983).
27. Ekerdt, J. G., Lapinski, M. P., and Campione, T. J., presented at the 193rd National Meeting of the American Chemical Society, Denver, CO, April 1987.
28. Davis, S. M., and Somorjai, G. A., *J. Phys. Chem.* **87,** 1545 (1983).
29. Mintsa-Eya, V., Touroude, R., and Gault, F. G., *J. Catal.* **66,** 412 (1980).
30. Sheppard, N., and Erkelens, J., *Appl. Spectrosc.* **38,** 471 (1984).
31. Boudart, M., and Djega-Mariadassou, G., "Kinetics of Heterogeneous Catalytic Reactions." Princeton Univ. Press, Princeton, NJ, 1984.
32. Greenler, R. G., Snider, D. R., Witt, D., and Sorbello, R. S., *Surf. Sci.* **118,** 415 (1982).
33. Jones, R. N., *Spectrochim. Acta* **9,** 235 (1957).
34. Koestner, R. J., Frost, J. C., Stair, P. C., Van Hove, M. A., and Somorjai, G. A., *Surf. Sci.* **116,** 85 (1982).
35. Koestner, R. J., Van Hove, M. A., and Somorjai, G. A., *J. Phys. Chem.* **87,** 203 (1983).
36. Machiels, C. J., and Anderson, R. B., *J. Catal.* **58,** 260 (1979).